Simulating study of atmospheric corrosion of steels in a coastal industrial zone: Effect of SO_3^{2-} on the formation of β-FeOOH rust particles synthesized from $FeCl_3$ solutions

Hidekazu Tanaka,[a*] Masahiko Inoue,[a] Tatsuo Ishikawa[b], Takenori Nakayama[c]

[a] Department of Chemistry, Graduate School of Science and Engineering, Shimane University,
1060 Nishikawatsu, Matsue, Shimane 690-8504, Japan

[b] School of Chemistry,
Osaka University of Education,
4-698-1 Asahigaoka, Kashiwara, Osaka 582-8582, Japan

[c] Materials Research Laboratory,
Kobe Steel, LTD.,
5-5 Takatsukadai 1, Nishi-ku, Kobe, Hyogo 651-2271, Japan

* responsible author

The name and address of the responsible author;
Dr. Hidekazu Tanaka
Department of Chemistry, Graduate School of Science and Engineering
Shimane University
1060 Nishikawatsu, Matsue, Shimane 690-8504
Japan
E-mail: hidekazu@riko.shimane-u.ac.jp
FAX: +81-852-32-6823

Abstract

For simulation of the atmospheric corrosion of steel in a coastal industrial district, β-FeOOH rusts were synthesized by aging the aqueous $FeCl_3$ solutions containing SO_3^{2-}. The yield and crystallite size of β-FeOOH were remarkably decreased by adding SO_3^{2-}, implying the suppression of formation and crystallization of β-FeOOH. Before aging, added SO_3^{2-} broke the coordination of Cl^- and OH^- to Fe^{3+} in Fe^{3+}-complexes and reduced the Fe^{3+} to Fe^{2+}. These facts suppose that SO_3^{2-} generated by dissolution of SO_X gas in thin film water on the steels at a coastal industrial zone markedly inhibits the formation of β-FeOOH rust.

Keywords: A. Steel; A. Iron; B. X-ray diffraction; C. Atmospheric corrosion; C. Rust

1. Introduction

Atmospheric corrosion of steels forms various kinds of steel rusts such as iron oxyhydroxides (α-, β- and γ-FeOOH), Fe_3O_4, poorly crystallized iron oxides and so forth. Among them, structure and composition of FeOOH rusts are strongly dependent of the exposure environment of steel [1-4]. The β-FeOOH rust is formed in Cl^--containing environment such as coastal and marine zones [1-2]. While, the α- and γ-FeOOH rusts are generated in urban and industrial zones including SO_X and NO_X in atmosphere [4]. This difference can be explained by considering that the Cl^-, SO_4^{2-} and NO_3^- respectively produced by dissolution of air-borne salt, SO_X and NO_X in thin film water on the steels markedly affect on the formation and composition of steel rusts [1-3]. Therefore, studying the influence of anions on the formation and structure of steel rusts is necessary to understand the atmospheric corrosion mechanism of steels. In particular, investigation of formation of β-FeOOH rust in the presence of anions generated from SO_X and NO_X is considerably important because major industrial districts of the world are developed at a coastal area. It is well-known that major components of SO_x and NO_x are SO_2 and NO_2, respectively, and dissolution of these gases in thin film water on the steels leads to the following reactions [3]:

$$SO_2 + H_2O \rightarrow HSO_3^- + H^+ \text{ ---(1)}$$

$$HSO_3^- \rightarrow SO_3^{2-} + H^+ \text{ ---(2)}$$

$$SO_3^{2-} + 1/2O_2 \rightarrow SO_4^{2-} \text{ ---(3)}$$

$$NO_2 + H_2O \rightarrow NO_3^- + 2H^+ \text{ ---(4)}$$

The corrosion behavior and rust formation of steel have been examined by exposure test in marine atmosphere containing SO_2 [5-12]. However, a little study has been done about the influence of SO_4^{2-} and NO_3^- on the formation of β-FeOOH rust [13-21]. Oh et al. indicated by preparation of rust particles in a mixture of $FeCl_2$ and $FeSO_4$ solutions that increasing molar ratio $[SO_4^{2-}]/[Cl^-]$

enhances the α-FeOOH formation [14]. Ishikawa et al. and Kamimura et al. reported that the formation and crystallization of β-FeOOH particles are suppressed by addition of SO_4^{2-} and this behavior is associated with the stability of coordination of anions to Fe^{3+} in Fe^{3+}-complexes [16,17]. Also, the authors synthesized the steel rust particles in a mixture of aqueous $FeCl_3$, $Fe_2(SO_4)_3$ and $Fe(NO_3)_3$ solutions and revealed that the SO_4^{2-} markedly inhibits the β-FeOOH formation, while no remarkable effect of NO_3^- is recognized [19]. Similar results were found for the steel rust particles prepared by aerial oxidation of a mixture of aqueous $FeCl_2$, $FeSO_4$ and $NaNO_3$ solutions [20,21]. On the other hand, sulfite ions (SO_3^{2-}) generated by reaction (2) have almost not received attention in rust formation because the SO_3^{2-} is finally oxidized to SO_4^{2-} via reaction (3). Nonetheless, since the stability of coordination of SO_3^{2-} to Fe^{3+} in Fe^{3+}-complexes is higher than that of SO_4^{2-} [22], SO_3^{2-} would affect on the formation of β-FeOOH rust as well as SO_4^{2-}.

The aim of this study was to clarify the effect of SO_3^{2-} on the formation and structure of β-FeOOH rust. So that, the β-FeOOH particles were synthesized by aging the aqueous $FeCl_3$ solutions containing different amounts of Na_2SO_3, and the formation and structure of the products were examined by various means. The results obtained must serve to elucidate the atmospheric corrosion mechanism of steels in a coastal industrial zone.

2. Experimental

2.1 Synthesis of β-FeOOH particles in the presence of SO_3^{2-}

The β-FeOOH particles were synthesized by hydrolysis of aqueous $FeCl_3$ solutions as follows. Aqueous solutions (250 mL) dissolving 0.03 mol of $FeCl_3$ were prepared in a sealed polypropylene vessel. To the $FeCl_3$ solutions, aqueous solutions (50 mL) dissolving various amounts of Na_2SO_3 were added.

Then, molar ratio SO_3^{2-}/Fe^{3+} in the solution ranged from 0 to 0.4 and the Fe^{3+} concentration was 100 mmol/L. The solutions thus prepared were aged at 85°C for 24 h in an air oven without stirring. The resulting precipitates were filtered off using 0.45 μm Millipore filter, fully washed with deionized-distilled water and finally dried in an air oven at 50°C for 24 h. All the chemicals purchased from Wako Pure Chemical Co. were regent grade and used without further purification.

2.2 Characterization

The samples thus obtained were characterized by a variety of conventional techniques. Powder X-ray diffraction (XRD) patterns were taken by a Rigaku diffractometer with a Ni-filtered Cu*K*α radiation at 30 kV and 15 mA. Particle morphology was observed by a TOPCON transmission electron microscope (TEM) at 200 kV. UV spectra were measured by a Shimadzu UV-vis spectrometer and quartz cell. Fe^{2+} concentration in the solution was assayed by an *o*-phenanthroline color comparison method.

3. Results and Discussion

Fig. 1 plots yield of the product as a function of molar ratio SO_3^{2-}/Fe^{3+}. It is clearly seen that yield of the product linearly decreases with the increase of SO_3^{2-}/Fe^{3+} ratio and reaches to zero at $SO_3^{2-}/Fe^{3+} \geq 0.3$. This fact indicates that added SO_3^{2-} strongly suppresses the formation of β-FeOOH rusts.

Fig. 2 shows the XRD patterns of the products prepared at different SO_3^{2-}/Fe^{3+} ratios. At $SO_3^{2-}/Fe^{3+} = 0$, the diffraction peaks due to β-FeOOH (PDF no. 34-1266) mainly develop at 2θ = 11.8°, 16.8°, 26.6°, 34.1°, 35.1°, 39.0°, 46.3° and 55.9°, corresponding to the reflection from (101), (200), (301), (004), (211), (310), (114) and (215) planes of the crystal (pattern **a**). Besides, the peaks

related to secondary phase are not detected. On raising SO_3^{2-}/Fe^{3+} ratio, the peaks characteristics of β-FeOOH are gradually weakened and broadened, while the position of the peaks is unchanged (patterns **b** - **f**). Furthermore, weak peaks due to α-FeOOH (no. 81-464) appear at SO_3^{2-}/Fe^{3+} = 0.15 and are intensified with an increment of SO_3^{2-}/Fe^{3+} ratio (patterns **d** – **f**). Fig. 3 plots the crystallite size of β-FeOOH evaluated from full width at half maximum of the (301) peak at 2θ = 26.6° using the Scherrer equation against molar ratio SO_3^{2-}/Fe^{3+}. The crystallize size is 106 nm at SO_3^{2-}/Fe^{3+} = 0 and is dramatically decreased by raising SO_3^{2-}/Fe^{3+} ratio. From these results, it is most likely that formation and crystallization of β-FeOOH are markedly impeded by addition of SO_3^{2-}.

Fig. 4 shows the TEM pictures of the particles synthesized at various molar ratios SO_3^{2-}/Fe^{3+}. The rod-shaped β-FeOOH particles are observed at SO_3^{2-}/Fe^{3+} = 0 and their mean particle length and width are 278 nm and 61 nm, respectively (picture **a**). The size of β-FeOOH particles slightly decreases as SO_3^{2-}/Fe^{3+} ratio increases to 0.1, meaning the suppression of growth of the particles by added SO_3^{2-} (pictures **b** and **c**). At $SO_3^{2-}/Fe^{3+} \geq 0.15$, the size of β-FeOOH particles increases and the irregular particles with a size of ca. 20 nm are formed (pictures **d** – **f**). The irregular particles would be identified as α-FeOOH because the formation of this material is recognized at the same SO_3^{2-}/Fe^{3+} ratio by XRD measurements shown in Fig. 2.

The foregoing results indicate that the SO_3^{2-} generated by dissolution of SO_X gas in thin film water on the steels at a coastal industrial atmosphere remarkably inhibits the formation and crystallization of β-FeOOH rust.

It is well-known that formation of iron oxyhydroxide particles such as β-FeOOH is dependent of the solution pH [1,4,23,24]. Hence, pH of the solution before aging is plotted as a function of SO_3^{2-}/Fe^{3+} ratio in Fig. 5. Clearly seen that the

solution pH before aging gradually decreases on raising SO_3^{2-}/Fe^{3+} ratio. Besides, increment of SO_3^{2-}/Fe^{3+} ratio changes the color of the solution from light yellow to orange without forming any precipitates as shown in Fig. 5. These facts allow us to infer that added SO_3^{2-} alters the coordination of anions to Fe^{3+} in Fe^{3+}-complexes. To make clearer of this, UV spectra of the solution before aging were measured. The results are displayed in Fig. 6. At SO_3^{2-}/Fe^{3+} = 0, two absorption peaks appear around at 210 nm and 335 nm (spectrum **a**). The former and latter peaks are assignable to the coordination of OH^- and Cl^- to Fe^{3+} in Fe^{3+}-complexes, respectively [25,26]. It should be noted that these peaks are weakened by raising SO_3^{2-}/Fe^{3+} ratio (spectra **b** – **h**). Furthermore, at SO_3^{2-}/Fe^{3+} ≥ 0.15, new peak is found at ca. 305 nm and is identified as the coordination of SO_4^{2-} to Fe^{3+} in Fe^{3+}-complexes (spectra **d** – **h**) [25,26]. It seems, therefore, that added SO_3^{2-} breaks the coordination of OH^- and Cl^- to Fe^{3+} in Fe^{3+}-complexes. This can be explained by the difference of stability constant of Fe^{3+}-complexes with anions. The logarithm of stability constants (log *K*) of Fe^{3+}-complexes with OH^- and Cl^- are -2.9 and 0.6, respectively [22]. On the other hand, SO_3^{2-} forms a stable coordination to Fe^{3+} compared with OH^- and Cl^- [22]. Nevertheless, no peak characteristics due to coordination of SO_3^{2-} to Fe^{3+} can be found in all of the UV spectra. It is well-known that Na_2SO_3 is a strong reducing agent and is widely used as preservatives. Further, López-Miranda et al. reported the preparation of Ag nanoparticles in aqueous $AgNO_3$ solution using Na_2SO_3 as a reducing agent [27]. It seems, therefore, that Fe^{3+} in the solution before aging is reduced to Fe^{2+} by added SO_3^{2-}. To elucidate this, Fe^{2+} concentration ($[Fe^{2+}]$) in the solution before aging was assayed by an *o*-phenanthroline color comparison method. Also, Fe^{3+} concentration ($[Fe^{3+}]$) was calculated by subtracting from 100 mmol/L of initial $[Fe^{3+}]$ to assayed $[Fe^{2+}]$. Fig. 7 plots the $[Fe^{2+}]$ and $[Fe^{3+}]$ in the solution before aging, respectively represented by open and filled circles,

against molar ratio SO_3^{2-}/Fe^{3+}. Note that raising SO_3^{2-}/Fe^{3+} ratio linearly increases the $[Fe^{2+}]$ and decreases the $[Fe^{3+}]$, being indicative of the reduction of Fe^{3+} to Fe^{2+} by addition of SO_3^{2-}. Further, amount of formed Fe^{2+} in the solution is about twice as large as amount of Fe^{3+}. This means that one SO_3^{2-} ion reduces two Fe^{3+} ions and almost all the added SO_3^{2-} reacts with Fe^{3+}.

From these results, we can suppose the influence of SO_3^{2-} on the formation of β-FeOOH rust. The formation of iron rust particles in acidic Fe^{3+} solution was reported as follows [23,24,28]. The hexa-aqua ferric ions are produced by the reaction of Fe^{3+} with H_2O via reaction (5).

$$Fe^{3+} + 6H_2O \quad \square \quad [Fe(H_2O)_6]^{3+} \text{ ---(5)}$$

The $[Fe(H_2O)_6]^{3+}$ is hydrolyzed to form $[Fe(OH)_n(H_2O)_{6-n}]^{3+}$ (n = 1 – 6) via protolysis reaction (6).

$$[Fe(H_2O)_6]^{3+} + nH_2O \quad \square \quad [Fe(OH)_n(H_2O)_{6-n}]^{3+} + nH_3O^+ \text{ ---(6)}$$

The >Fe-OH groups of the $[Fe(OH)_n(H_2O)_{6-n}]^{3+}$ are condensed via oxolation reaction (7).

$$>Fe\text{-}OH + HO\text{-}Fe< \quad \square \quad >Fe\text{-}O\text{-}Fe< + H_2O \text{ ---(7)}$$

Also, the >Fe-OH groups of the $[Fe(OH)_n(H_2O)_{6-n}]^{3+}$ react with >Fe-H_2O groups via olation reaction (8).

$$>Fe\text{-}OH + H_2O\text{-}Fe< \quad \square \quad >Fe\text{-}OH\text{-}Fe< + H_2O \text{ ---(8)}$$

The reactions (5) – (8) continuously progress during aging to form various kinds of iron rust particles. UV measurement of the solution before aging at SO_3^{2-}/Fe^{3+} = 0 found the coordination of OH^- and Cl^- to Fe^{3+} in Fe^{3+}-complexes, meaning the formation of $[Fe(OH)_nCl_m(H_2O)_{6-n-m}]^{3+}$ by reaction (9):

$[Fe(H_2O)_6]^{3+} + nH_2O + mCl^- \square [Fe(OH)_nCl_m(H_2O)_{6-n-m}]^{3+} + nH_3O^+ + mH_2O$ ---(9).

Therefore, the protolysis, oxolation and olation reactions of $[Fe(OH)_nCl_m(H_2O)_{6-n-m}]^{3+}$ proceed during aging to crystallize as Cl^--containing β-FeOOH. When the SO_3^{2-} is added in the solution before aging, the SO_3^{2-}

breaks the coordination of OH^- and Cl^- to Fe^{3+} in $[Fe(OH)_nCl_m(H_2O)_{6-n-m}]^{3+}$ and reduces the Fe^{3+} to Fe^{2+} via reaction (10), because the stability constant of Fe^{3+}-complex with SO_3^{2-} is much higher than that with Cl^- and OH^- [22]:

$$2Fe^{3+} + SO_3^{2-} + H_2O \quad --> \quad 2Fe^{2+} + SO_4^{2-} + 2H^+ \text{ ---(10).}$$

The reaction (10) falls the solution pH, corresponding to the change of solution pH before aging against SO_3^{2-}/Fe^{3+} ratio shown in Fig. 5. It has been established that decrease of solution pH lowers the hydrolysis rate of Fe^{3+} and oxidation rate of Fe^{2+} [29]. Therefore, the Fe^{2+} formed by reaction (10) is difficult to oxidize to Fe^{3+}. As a result, the addition of SO_3^{2-} remarkably suppresses the formation and crystallization of β-FeOOH rust and the effect is enhanced on elevating SO_3^{2-}/Fe^{3+} ratio. Also, a slight amount of α-FeOOH particles is generated in addition to β-FeOOH ones by adding SO_3^{2-}. As stated above, almost all the SO_3^{2-} is oxidized to SO_4^{2-} via reaction (10). It seems, therefore, that the α-FeOOH formation is related to the generated SO_4^{2-} because the stability constant of Fe^{3+}-complex with SO_4^{2-} (4.1) is much larger than that with Cl^- and OH^- [22]. Hence, the yielded SO_4^{2-} preferentially coordinates to Fe^{3+} to form stable Fe^{3+}-complex such as $[Fe(OH)_n(SO_4)_{m/2}(H_2O)_{6-n-m}]^{3+}$. It has been reported that formation of SO_4^{2-}-containing Schwertmannite ($Fe_8O_8(OH)_6(SO_4)$) is formed by aging the $[Fe(OH)_n(SO_4)_{m/2}(H_2O)_{6-n-m}]^{3+}$ in acidic solution and the material is transformed into α-FeOOH [19-21,30-34]. Accordingly, the Schwertmannite particles are initially formed by adding SO_3^{2-} and are transformed into irregular-shaped α-FeOOH ones during aging.

From the above-mentioned results, it is indicative that the SO_3^{2-} generated from corrosive SO_X gas in a coastal industrial atmosphere strongly suppresses the formation and crystallization of β-FeOOH rust on the steels.

4. Conclusions

From the information presented in this publication, following conclusions can be drawn. The yield of the products steeply decreased on elevating SO_3^{2-}/Fe^{3+} ratio and reaches to zero at $SO_3^{2-}/Fe^{3+} \geq 0.3$. Also, increment of SO_3^{2-}/Fe^{3+} ratio markedly lowered the crystallite size of β-FeOOH. These results indicate the suppression of formation and crystallization of β-FeOOH rust by adding SO_3^{2-}. This could be identified as the change in coordination of anions to Fe^{3+} in Fe^{3+}-complexes in the solution before aging by addition of SO_3^{2-}. At $SO_3^{2-}/Fe^{3+} = 0$, the coordination of OH^- and Cl^- to Fe^{3+} in Fe^{3+}-complexes was recognized. Added SO_3^{2-} broke the coordination of OH^- and Cl^- to Fe^{3+} because the coordination of SO_3^{2-} to Fe^{3+} in Fe^{3+}-complex is more stable than that of Cl^- and OH^-. Further, added SO_3^{2-} reduces the Fe^{3+} to Fe^{2+} as following reaction: $2Fe^{3+} + SO_3^{2-} + H_2O \rightarrow 2Fe^{2+} + SO_4^{2-} + 2H^+$. As a result, $[Fe^{3+}]$ in the solution and solution pH were decreased, leading to the inhibition of formation and crystallization of β-FeOOH rust particles.

The obtained results infer that SO_3^{2-} produced by dissolution of corrosive SO_X gas in thin film water on the steels at a coastal industrial zone markedly suppresses the formation and crystallization of β-FeOOH rust.

Acknowledgements

The authors grateful thank to Mr. Tsunao Yoneyama of Department of Biosignaling and Radioisotope Experiment Center for Integrated Research in Science of Shimane University for his help with TEM observation. This study was partly supported by the Grant-in-Aid for Young Scientists Fund (B) (23760699) and Scientific Research (C) (26420739).

References

[1] W. Feitknecht, Chem. Ind. 36 (1959) 1102-1109.

[2] P. Keller, Werkst. Korros. 20 (1969) 102-108.

[3] C. Leygraf, T.E. Graedel, Atmospheric Corrosion, John Wiley & Sons, New York, 2000.

[4] J.D. Bernal, D.R. Dasgupta, A.L. Mackay, Clay Miner. Bull. 4 (1959) 15-30.

[5] S.J. Oh, D.C. Cook, H.E. Townsend, Corros. Sci. 41 (1999) 1687-1702.

[6] Y. Ma, Y. Li, F. Wang, Corros. Sci. 51 (2009) 997-1006.

[7] J.G. Castaño, C.A. Botero, A.H. Restrepo, E.A. Agudelo, E. Correa, F. Echeverría, Corros. Sci. 52 (2010) 216-223.

[8] D. de la Fuente, I. Díaz, J. Simancas, B. Chico, M. Morcillo, Corros. Sci. 53 (2011) 604-617.

[9] Z. Wang, J. Liu, L. Wu, R. Han, Y. Sun, Corros. Sci. 76 (2013) 1-10.

[10] I. Diaz, H. Cano, D. de la Fuente, B. Chico, J.M. Vega, M. Morcillo, Corros. Sci. 76 (2013) 348-360.

[11] W. Chen, L. Hao, J. Dong, W. Ke, Corros. Sci. 83 (2014) 155-163.

[12] J. Alcántara, B. Chico, I. Díaz, D. de la Fuente, M. Morcillo, Corros. Sci. 97 (2015) 74-88.

[13] S. Misawa, K. Hashimoto, S. Shimodaira, Corros. Eng. 23 (1974) 17-27.

[14] S.J. Oh, S.-J. Kwon, J.-Y. Lee, J.-Y. Yoo, W.Y. Choo, Corrosion 58 (2002) 498-504.

[15] C. Sudakar, G.N. Subbanna, T.R.N. Kutty, J. Phys. Chem. Solids 64 (2003) 2337-2349.

[16] T. Ishikawa, S. Miyamoto, K. Kandori, T. Nakayama, Corros. Sci. 47 (2005) 2510-2520.

[17] T. Kamimura, S. Nasu, T. Segi, T. Tazaki, H. Miyuki, S. Morimoto, T. Kudo, Corros. Sci. 47 (2005) 2531-2542.

[18] A.A. Al-Refaie, J. Walton, R.A. Cottis, R. Lindsay, Corros. Sci. 52 (2010) 422-428.

[19] H. Tanaka, N. Hatanaka, M. Muguruma, T. Ishikawa, T. Nakayama, Corros. Sci. 66 (2013) 136-141.

[20] H. Tanaka, N. Hatanaka, M. Muguruma, A. Nishitani, T. Ishikawa, T. Nakayama, J. Soc. Powder Technol. Japan 52 (2015) 4-9.

[21] H. Tanaka, J. Soc. Powder Technol. Japan 52 (2015) 398-404.

[22] L.G. Sillen, A.E. Martell, Stability Constants of Metal-Ion Complexes, The Chemical Society, London, 1964.

[23] R.M. Cornell, U. Schwertmann, The Iron Oxides, VCS, Weinheim, 1996.

[24] H. Tamura, Corros. Sci. 50 (2008) 1872-1883.

[25] E. Rabinowitch, W.H. Stockmayer, J. Am. Chem. Soc. 64 (1942) 335-347.

[26] D.M. Sherman, T.D. Waite, Amer. Mineral. 70 (1985) 1262-1269.

[27] A. López-Miranda, A. López-Valdivieso, G. Viramontes-Gamboa, J. Nanopart Res. 13 (2012) 1101-1111.

[28] M. Schultz, W. Burckhardt, S.T. Barth, J. Mater. Sci. 34 (1999) 2217-2227.

[29] B. Morgan, O. Lahav, Chemosphere 68 (2007) 2080-2084.

[30] J.M. Bigham, U. Schwertmann, S.J. Traina, R.L. Winland, M. Wolf, Geochim. Cosmochim. Ac. 60 (1996) 2111-2121.

[31] U. Schwertmann, L. Carlson, Clay Miner. 40 (2005) 63-66.

[32] E.D. Burton, R.T. Bush, L.A. Sullivan, D.R.G. Mitchell, Geochim. Cosmochim. Ac. 72 (2008) 4551-4564.

[33] S. Paikaray, S. Peiffer, Appl. Geochem. 27 (2012) 590-597.

[34] M. Muguruma, H. Tanaka, T. Ishikawa, T. Nakayama, Zairyo-to-Kankyo 64 (2015) 235-239.

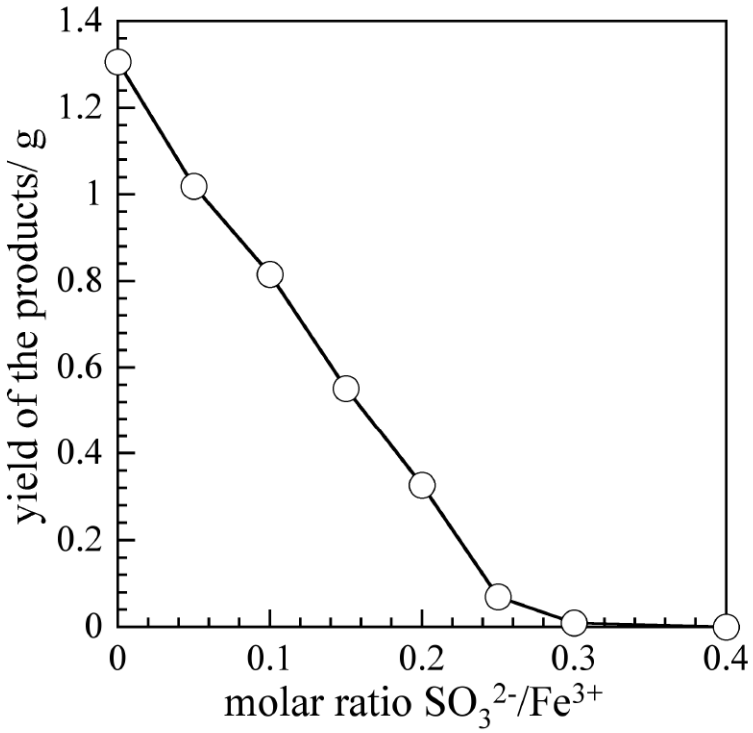

Fig. 1. Plots of yield of the β-FeOOH prepared at 85°C for 24 h as a function of molar ratio SO_3^{2-}/Fe^{3+}.

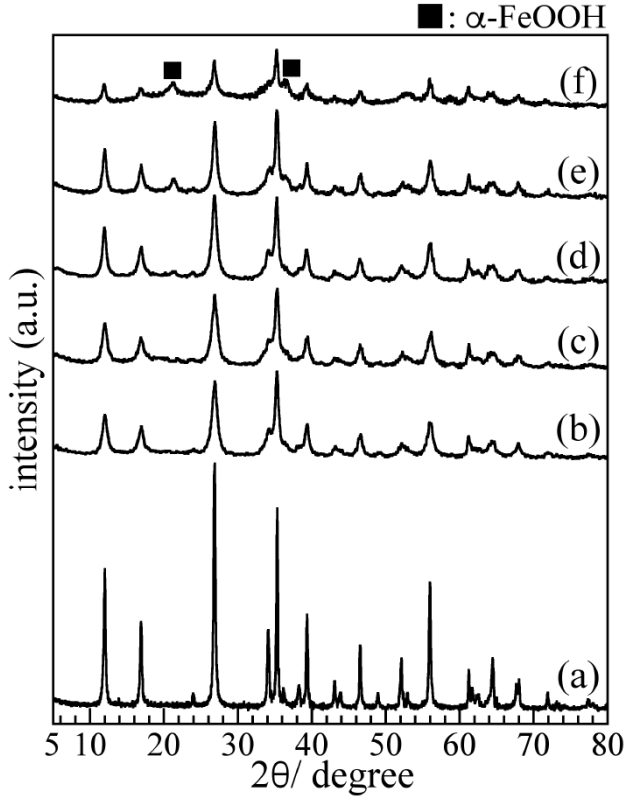

Fig. 2. XRD patterns of β-FeOOH prepared at different SO_3^{2-}/Fe^{3+} ratios and 85°C for 24 h. SO_3^{2-}/Fe^{3+} ratio: (a) 0, (b) 0.05, (c) 0.1, (d) 0.15, (e) 0.2, (f) 0.25.

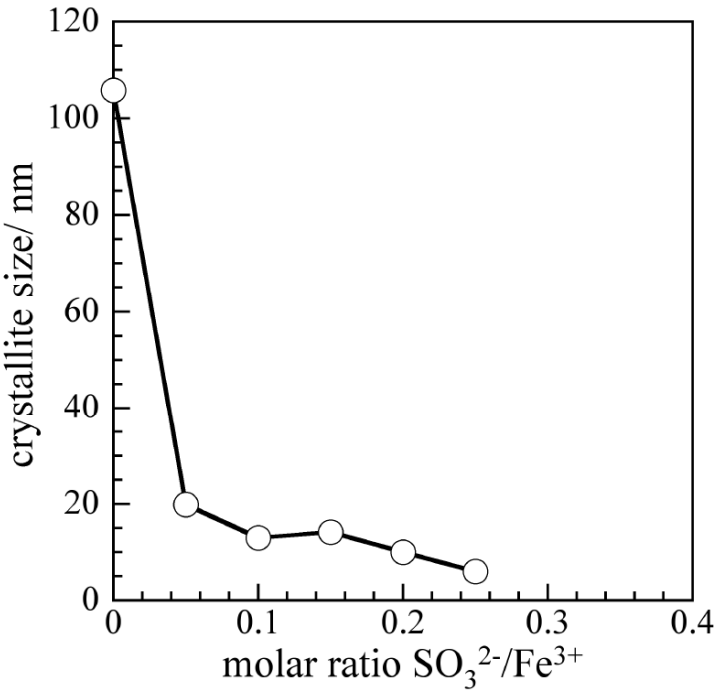

Fig. 3. Plots of crystallite size of β-FeOOH prepared at 85°C for 24 h against molar ratio SO_3^{2-}/Fe^{3+}.

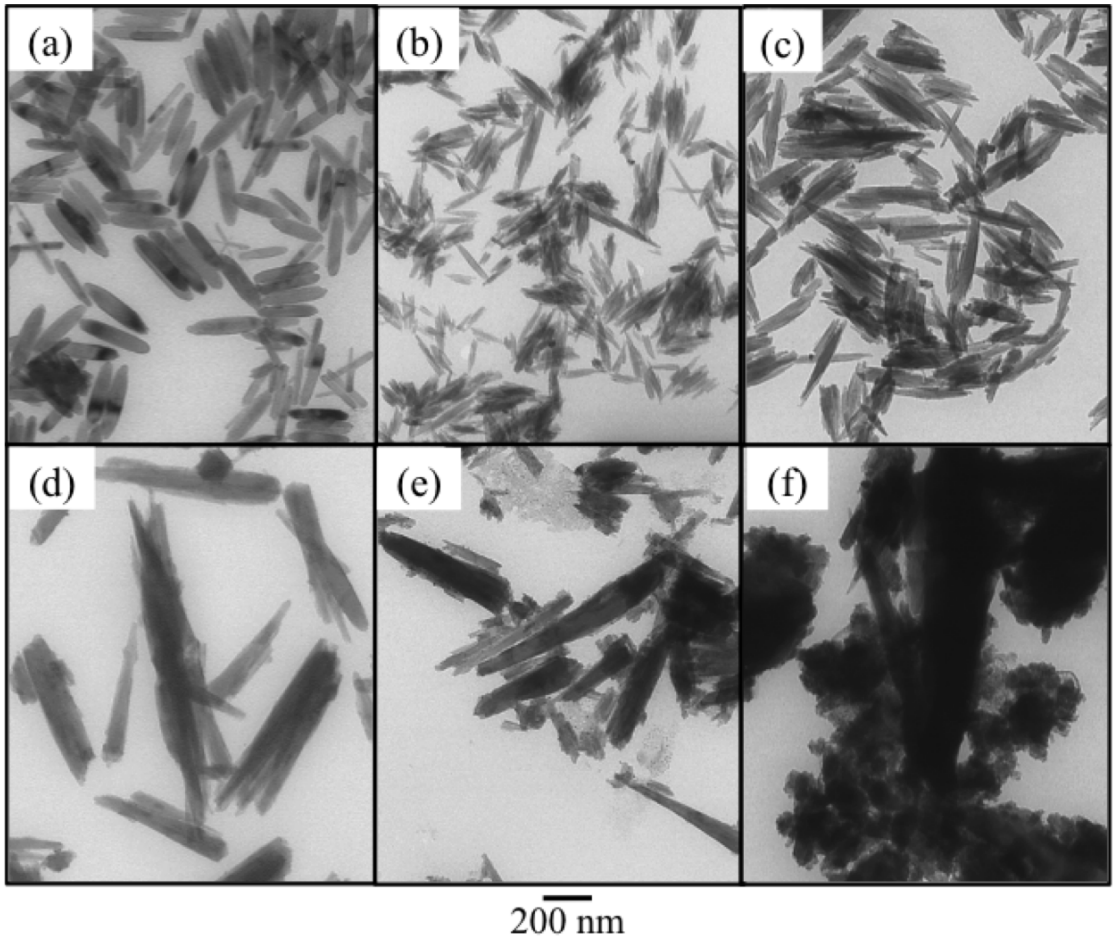

Fig. 4. TEM pictures of β-FeOOH particles prepared at different SO_3^{2-}/Fe^{3+} ratios and 85°C for 24 h. SO_3^{2-}/Fe^{3+} ratio: (a) 0, (b) 0.05, (c) 0.1, (d) 0.15, (e) 0.2, (f) 0.25.

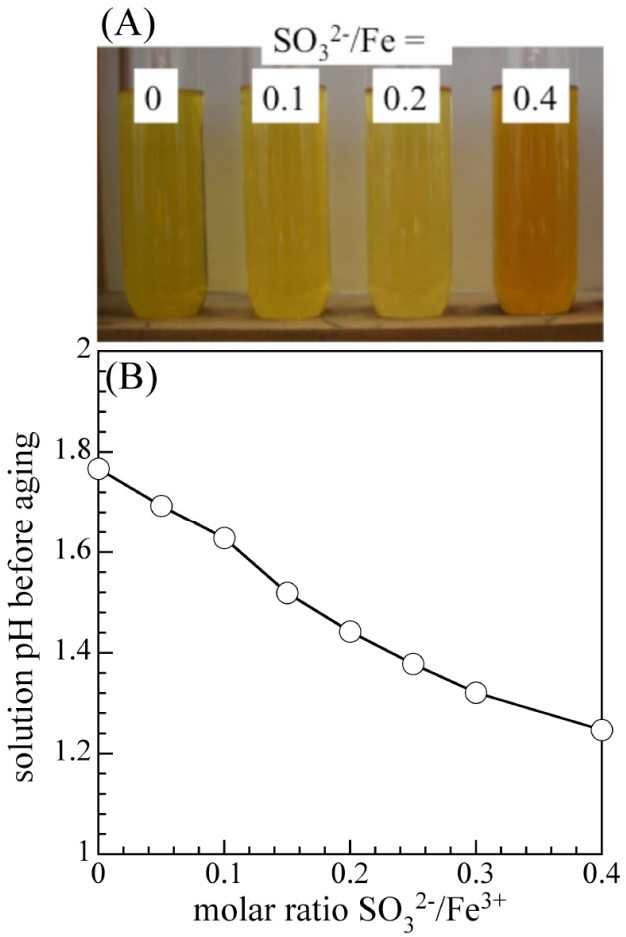

Fig. 5. (A) Picture of the solution before aging at different SO_3^{2-}/Fe^{3+} ratios and (B) plots of solution pH before aging as a function of molar ratio SO_3^{2-}/Fe^{3+}.

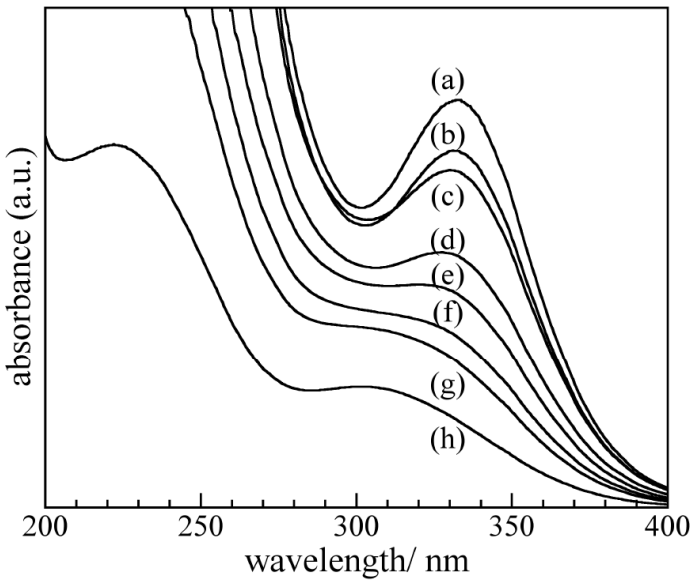

Fig. 6. UV spectra of the solution before aging at different SO_3^{2-}/Fe^{3+} ratios. SO_3^{2-}/Fe^{3+} ratio: (a) 0, (b) 0.05, (c) 0.1, (d) 0.15, (e) 0.2, (f) 0.25, (g) 0.3, (h) 0.4.

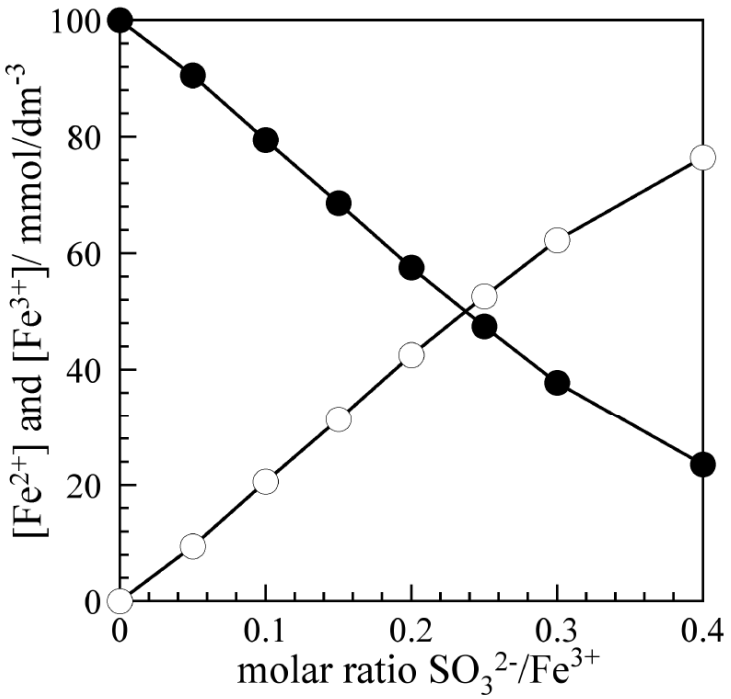

Fig. 7. Plots of (○) $[Fe^{2+}]$ and (●) $[Fe^{3+}]$ in the solution before aging as a function of molar ratio SO_3^{2-}/Fe^{3+}.